Available online at www.sciencedirect.com
SCIENCE DIRECT®
Journal of Solid State Chemistry 177 (2004) 1285–1291
JOURNAL OF SOLID STATE CHEMISTRY
http://elsevier.com/locate/jssc

Crystal structures and magnetic properties of $CaSb_xMn_{1-x}O_3$ perovskites

Victor Poltavets,[a] K. Vidyasagar,[b] and Martin Jansen[a,*]

[a] *Max-Planck Institut für Festkörperforschung, Heisenbergstr. 1, Stuttgart 70569, Germany*
[b] *Department Chemistry, Indian Institute of Technology Madras, Chennai 600036, India*

Received 5 June 2003; received in revised form 29 October 2003; accepted 6 November 2003

Abstract

Manganese perovskites of the $CaSb_xMn_{1-x}O_3$ ($x = 0.1, 0.2, 0.25, 0.33, 0.5$) family have been synthesized by solid state reactions and structurally characterized by Rietveld refinement of the powder X-ray diffraction data. $CaSb_{0.1}Mn_{0.9}O_3$ crystallizes in *Pnma* space group with a $GdFeO_3$-type orthorhombic structure, whereas the other members of the series crystallize in the space group $P2_1/m$. Unit cell volumes of these members increase linearly with antimony content. Divergences between ZFC and FC magnetic susceptibilities were observed for $CaSb_{0.1}Mn_{0.9}O_3$, $CaSb_{0.33}Mn_{0.67}O_3$ and $CaSb_{0.5}Mn_{0.5}O_3$ at low temperatures. Antiferromagnetic transitions at 125 K and 113 K were found for $CaSb_{0.2}Mn_{0.8}O_3$ and $CaSb_{0.25}Mn_{0.75}O_3$, respectively.

Keywords: Manganese perovskites; Substitution of manganese; Distorted perovskites; Magnetic clusters

1. Introduction

Manganese oxides with the perovskite structure are known to exhibit anomalous magnetic and transport properties [1]. The colossal magnetoresistance (CMR) effect in these materials [2,3] has been extensively investigated during the last decade. However, the mechanism of CMR is not yet completely understood. The importance of the static Jahn–Teller distortion of the Mn^{3+} centers and the double exchange mechanism between the Mn^{3+} and the Mn^{4+} ions in these oxides has been well-recognized [4]. A possible existence of noncollinear magnetic structures, in intermediate concentrations between antiferromagnetic and ferromagnetic states, was predicted on the basis of the double exchange theory [5]. The phase separation model with coexisting clusters of competing electronic phases has been already reviewed [6,7]. Experimental evidences of this model were obtained by means of X-ray absorption [8], NMR [9], neutron scattering [10], electron microscopy [11], scanning tunneling spectroscopy [12] and other methods. The simultaneous presence of different kinds of clusters complicates the comprehension of properties of these oxides. The behavior of the clusters cannot be predicted from the comparison between the analogous bulk phases. Therefore, investigation of some model perovskites, in which clusters of only one electronic phase are stabilized, could be useful for the understanding of the CMR phenomena.

Such model perovskites could be formed by partial substitution of manganese with some nonmagnetic ions in stable oxidation states. This would diminish long-range interactions between the manganese ions and possibly lead to the stabilization of magnetic clusters with dominant short-range interactions. The studies of substitutions of manganese with Mg^{2+} [13,14], Ti^{4+}, Nb^{5+} [13], Fe^{3+} [15], Al^{3+} [16], $Ru^{5+/4+}$ [17,18], Cr [16,19,20], Co, Ni [20], Mo^{6+} [18] have been reported. Such substitutions could induce lattice distortions, which should be minimum for a fair comparison of properties of phases with and without substitution at Mn position. From this point of view, the use of nonmagnetic Sb^{5+} ion, which is intermediate in size between Mn^{3+} and Mn^{4+} ions, could be considered for substitution. In this article, we report the crystal structures, magnetic and electrical resistivity properties of $CaSb_xMn_{1-x}O_3$ ($x = 0.1, 0.2, 0.25, 0.33, 0.5$) perovskite solid solutions.

*Corresponding author. Fax: +49-711-689-1502.
E-mail address: m.jansen@fkf.mpg.de (M. Jansen).

0022-4596/$ - see front matter © 2003 Elsevier Inc. All rights reserved.
doi:10.1016/j.jssc.2003.11.002

2. Experimental

Samples with $x = 0.1$, 0.2, 0.25, 0.33, 0.5 of the $CaSb_xMn_{1-x}O_3$ family were prepared by the conventional solid-state method. $CaCO_3$, Mn_2O_3 and Sb_2O_5 powders (purity 99.9%) were weighed in desired ratios and calcined in air at 900°C for 30 h. The products were then ground and annealed at 1200°C for 60 h with one intermittent grinding. Samples with $x = 0.33$ and 0.5 were heated further at 1400°C for 48 h with another intermittent grinding. All the five samples were finally annealed in oxygen at 600°C for 48 h. The syntheses of all samples and the consequent X-ray diffraction, magnetic and electrical resistivity measurements were successfully reproduced.

All the five solid solutions were ascertained, by energy dispersive X-ray analysis (Zeiss DMS 940, EDAX PV9800), to contain the metal ions in the desired, nominal ratios. The EDAX spectra were recorded at an acceleration energy of 25 keV and the Ca–K, Sb–L and Mn–K lines were used to calculate the cation concentration. The oxygen content was analyzed by standard iodometric titrations.

The X-ray powder diffraction patterns were recorded at room temperature by steps of 0.02° (2θ) on a Stoe Stadi P diffractometer equipped with a linear position sensitive detector and either monochromatic Cu$K\alpha_1$ or monochromatic Mo$K\alpha_1$ radiation. Silicon ($a = 5.43088(4)$ Å) was used as external calibration standard. The Rietveld refinements were carried out, based on the models for the distorted perovskites presented in the Woodwards article [21]. The programs FullProf.2k (version 2.00) [22] or Rietan-94 [23] were used to refine the crystal structures by the Rietveld [24] method. DRXWin [25] program was used as a complementary analytical and graphical tool to facilitate the structural refinement. In the final runs of the Rietveld refinement, the following parameters were refined: scale factor, unit-cell parameters, profile shape parameters, asymmetry parameters, background coefficients, atomic positional coordinates and isotropic thermal factors. The quality of the agreement between observed and calculated profiles was monitored by a set of conventional R factors, as described by Young [26].

The magnetic susceptibility measurements were carried out on powder samples of perovskite oxides with a commercial SQUID magnetometer (QuantumDesign, MPMS-7.0) at different magnetic fields (0.01, 0.1, 1, and 5 T). All measurements were performed by warming the samples in the applied field after cooling to 2 K in zero field (ZFC, zero field cooling) and by cooling the samples in the measuring field (FC, field cooling). The molar magnetic susceptibilities were corrected for the diamagnetic contributions of each ion.

Measurements of the electrical resistivities were performed on sintered pellets of ca. 1 mm in height using a Hewlett-Packard 3457A multimeter. The resistivity data were obtained by the van der Pauw (four-point probe) method.

3. Results and discussion

All these oxygen-annealed samples have been found, by iodometric estimations, to be oxygen-deficient (Table 1). The results of chemical analysis were used to calculate the average manganese oxidation states in the specimens.

It has been found from the X-ray diffraction data, that the solid solution with $x = 0.1$ contains a small amount of admixture of unknown phases, whereas a very small quantity of $CaMn_2O_4$ is present in the sample with $x = 0.25$. Other solid solutions are essentially pure phases.

The Rietveld refinement of the XRD powder data of $CaSb_{0.1}Mn_{0.9}O_3$ was carried in the orthorhombic space group *Pnma*, in analogy with $CaMnO_3$ [27]. The observed, calculated and difference profiles of the Rietveld refinement X-ray diffraction data of $CaSb_{0.1}Mn_{0.9}O_3$ are plotted in Fig. 1. Lattice parameters are $a = 5.3096(1)$ Å ($\approx\sqrt{2}a_c$), $b = 7.5095(1)$ Å ($\approx 2a_c$) and $c = 5.3316(1)$ Å ($\approx\sqrt{2}a_c$) where a_c is edge-length of a simple cubic perovskite subcell. The relatively high value of R factor is due to overlap of a very small reflection of an unidentified admixture phase with the most intense reflection of the desired perovskite oxide. The final atomic parameters are given in Table 2. Our attempts of the Rietveld refinement of XRD powder data of $CaSb_{0.5}Mn_{0.5}O_3$, in *Pnma* space group were not satisfactory, as some of the small peaks revealed additional splitting. Refinement in monoclinic $P2_1/m$ space group was found to be successful with a good description of all peaks (Fig. 2, Table 3). Refinements in

Table 1
Pertinent data for $CaSb_xMn_{1-x}O_y$ solid solutions

Sb content, x	Oxygen content, y	Mn average oxidation state	Θ (K)	μ_{exp} ($\mu_B \cdot Mn^{-1}$)	μ_{calc} ($\mu_B \cdot Mn^{-1}$)
0.1	2.93	3.73	−26.78	4.27	4.17
0.2	2.92	3.55	−278.74	5.86	4.36
0.25	2.93	3.48	−206.30	5.73	4.44
0.33	2.90	3.21	−78.63	5.41	4.70
0.5	2.83	2.32	60.35	5.18	5.61

$P2_1/n$ space group, with either partial or complete ordering of the Sb and the Mn ions in the B positions [21] have been found to be not fruitful. The X-ray diffraction pattern of $CaSb_{0.33}Mn_{0.67}O_3$ was indexed with a monoclinic unit cell with $a = 5.348(1)$ Å, $b = 7.777(1)$ Å, $c = 5.363(1)$ Å and $\beta = 90.045(1)^\circ$. The diffraction peaks are substantially broader than those for samples with $x = 0.1$ and 0.5, probably due to local sample inhomogeneity. Rietveld refinements for samples with $x = 0.2$ and $x = 0.25$ were conducted in $P2_1/m$ space group (Figs. 3 and 4, Tables 4 and 5). Regions containing $CaMn_2O_4$ admixture reflections were excluded from the refinement, as they did not overlap with those of $CaSb_{0.25}Mn_{0.75}O_3$.

The perovskite solid solutions of the present study are distorted, from the ideal cubic perovskite structure, due to both tilting and deformation of $(Mn,Sb)O_6$ octahedra. Large deviations of the O–Mn–O bond angles from the ideal value of 90° were found across the entire $CaSb_xMn_{1-x}O_3$ series. Nevertheless, the structural description based on the rigid octahedral tilting [28] is still applicable. $CaSb_{0.1}Mn_{0.9}O_3$ adopts the structure with *Pnma* space group symmetry. The oxygen displacements from the ideal cubic perovskites positions can be approximated by a three-tilt system, $a^+b^-b^-$, which is commonly associated with the $GdFeO_3$ structure. Other members of the $CaSb_xMn_{1-x}O_3$ series adopt the $P2_1/m$ symmetry, which coincides with the $a^+b^-c^-$ tilt system [21]. The values of octahedral-rotation angles around [010] and [001] axes of the ideal cubic (aristotype) perovskite are equal in case of $a^+b^-b^-$ tilt system and different in the $a^+b^-c^-$ case. Further details of the crystal structure investigations can be obtained from the Fachinformationszentrum Karlsruhe, 76344 Eggenstein-Leopoldshafen, Germany, (fax: (49) 7247-808-666; e-mail: crysdata@fiz-karlsruhe.de) on quoting the depository number CSD-413158, CSD-413160, CSD-413159, CSD-413161 for samples with $x = 0.1$, 0.2, 0.25 and 0.5 correspondingly.

The relation between the cell volumes of $CaSb_xMn_{1-x}O_3$ and the composition (x) is shown in Fig. 5. A linear increase of the cell volume with increasing Sb concentrations is observed. The values of ionic radii of the octahedrally coordinated Sb^{5+}, Mn^{4+} and Mn^{3+} ions are 0.74 Å, 0.67 Å and 0.79 Å respectively [29]. Therefore, it is obvious that substitution of the Mn^{4+} by the Sb^{5+} in the $CaSb_xMn_{1-x}O_3$, and at the same time reducing the Mn^{4+} ions to the Mn^{3+}, result in the increase of the average ionic size in the B-position. Even larger Mn^{2+} ions with ionic radius of 0.97 Å are present in oxygen-deficient $CaSb_{0.5}Mn_{0.5}O_{2.83}$.

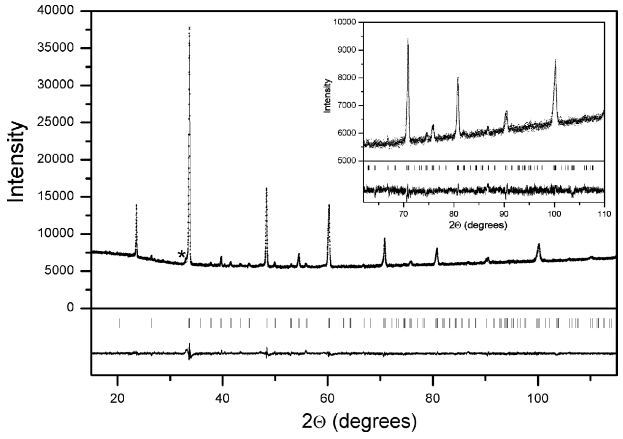

Fig. 1. Rietveld refinement profiles: observed (dots), calculated (solid lines), difference (bottom solid lines) and Bragg reflections (tick marks) for the fit to the X-ray powder pattern of the $CaSb_{0.1}Mn_{0.9}O_3$ perovskite. The main admixture peak is marked with * sign.

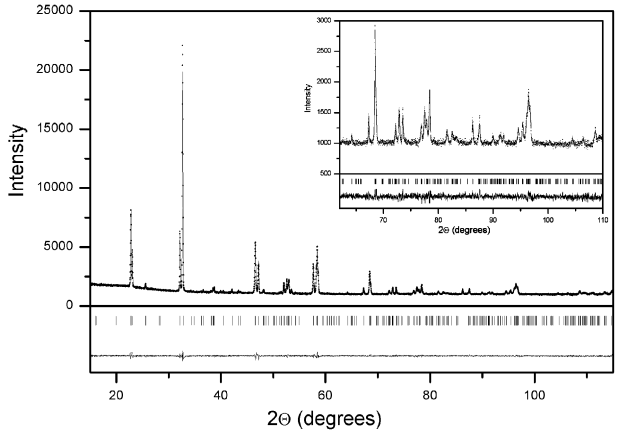

Fig. 2. Rietveld refinement profiles: observed (dots), calculated (solid lines), difference (bottom solid lines) and Bragg reflections (tick marks) for the fit to the X-ray powder pattern of the $CaSb_{0.5}Mn_{0.5}O_3$ perovskite.

Table 2
Results of the Rietveld refinement of $CaSb_{0.1}Mn_{0.9}O_3$ in the space group *Pnma* (No. 62)

Atom	Site	x/a	y/b	z/c	B_{iso} (Å^2)	Occupancy
Ca	4*c*	0.0003 (6)	0.25	0.0304 (5)	1.62 (4)	1
Mn/Sb	4*b*	0.5	0	0	0.83 (3)	0.9/0.1
O1	4*c*	−0.086 (2)	0.25	0.492 (3)	0.66 (7)[a]	1
O2	8*d*	0.297 (1)	−0.0265 (8)	0.283 (1)	0.66 (7)[a]	1

Note. Lattice parameters (Å): $a = 5.3096(1)$, $b = 7.5095(1)$, $c = 5.3316(1)$. R factors (%): $R_B = 10.1$, $R_{wp} = 12.7$, $R_F = 12.6$, $\chi^2 = 1.58$ (Cu$K\alpha_1$ radiation, refinement program: FullProf.2k).

[a] Parameters constrained to be equal.

Table 3
Results of the Rietveld refinement of $CaSb_{0.5}Mn_{0.5}O_3$ in the space group $P2_1/m$ (No. 11)

Atom	Site	x/a	y/b	z/c	B_{iso} (Å^2)	Occupancy
Ca1	2*e*	0.006 (2)	0.25	−0.055 (2)	1.6 (5)[a]	1
Ca2	2*e*	0.488 (2)	0.25	0.466 (2)	1.6 (5)[a]	1
Mn1/Sb1	2*b*	0.5	0	0	1.1 (2)	0.5/0.5
Mn2/Sb2	2*c*	0	0	0.5	0.5 (1)	0.5/0.5
O1	2*e*	−0.077 (5)	0.25	0.522 (3)	0.9 (1)[a]	1
O2	2*e*	0.604 (5)	0.25	0.037 (4)	0.9 (1)[a]	1
O3	4*f*	0.195 (2)	0.037 (3)	0.216 (3)	0.9 (1)[a]	1
O4	4*f*	0.290 (3)	0.058 (2)	0.690 (2)	0.9 (1)[a]	1

Note. Lattice parameters (Å): $a = 5.4624(1)$, $b = 7.6972(1)$, $c = 5.5590(1)$, $\beta = 90.090(2)$. *R* factors (%): $R_B = 5.0$, $R_{wp} = 11.2$, $R_F = 6.6$, $\chi^2 = 1.12$ (Cu$K\alpha_1$ radiation, refinement program: FullProf.2k).
[a] Parameters constrained to be equal.

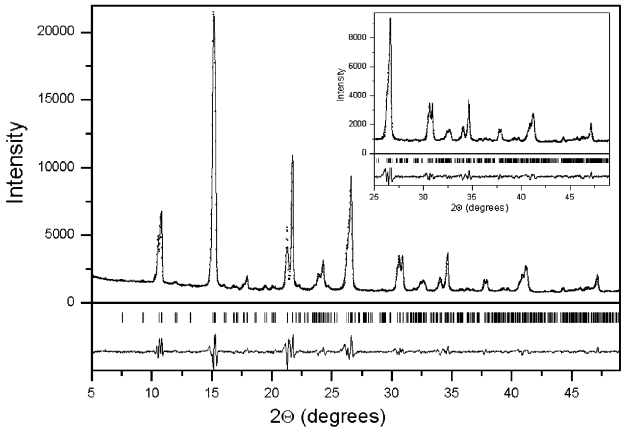

Fig. 3. Rietveld refinement profiles: observed (dots), calculated (solid lines), difference (bottom solid lines) and Bragg reflections (tick marks) for the fit to the X-ray powder pattern of the $CaSb_{0.2}Mn_{0.8}O_3$ perovskite.

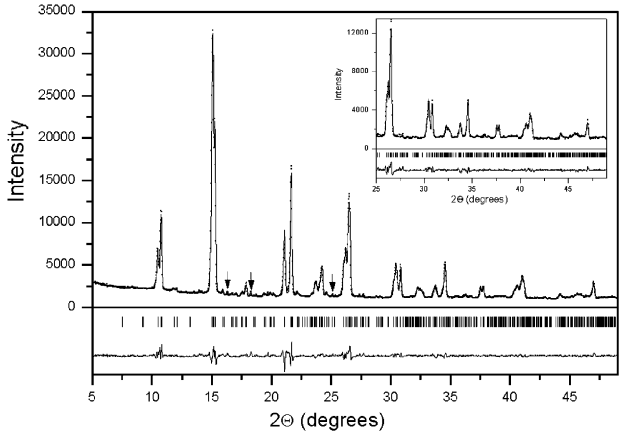

Fig. 4. Rietveld refinement profiles: observed (dots), calculated (solid lines), difference (bottom solid lines) and Bragg reflections (tick marks) for the fit to the X-ray powder pattern of the $CaSb_{0.25}Mn_{0.75}O_3$ perovskite. The arrows indicate the reflections of the impurity phase.

The molar magnetic susceptibility χ, corrected for core-diamagnetic contributions, is plotted versus temperature for all compositions (Fig. 6). The influence of admixtures on magnetic properties was estimated from the measurements made on different batches of the samples of a given compound. Magnetic transitions at 97 and 70 K, in a low magnetic field (0.01 T), were observed for the two trail batches of samples of $CaSb_{0.1}Mn_{0.9}O_3$. The magnitudes of the magnetic susceptibilities at 70 K are equal whereas the value at 97 K correlated well with the amount of admixture. Therefore, the transition at 97 K corresponds to the influence of the impurity and this transition could be almost totally suppressed by magnetic fields larger than 0.01 T. The antiferromagnetic transition at $T_N = 220$ K, corresponding to $CaMn_2O_4$ impurity [30], was not observed in all the $CaSb_{0.25}Mn_{0.75}O_3$ samples.

Divergences between the ZFC and FC measurements of magnetic susceptibility were observed for $CaSb_{0.1}Mn_{0.9}O_3$, $CaSb_{0.33}Mn_{0.67}O_3$ and $CaSb_{0.5}Mn_{0.5}O_3$. The observed field-dependence of transition temperatures suggests the formation of canted spin structures or spin glass. Antiferromagnetic transitions at T_N equal to 125 and 113 K were observed for $CaSb_{0.2}Mn_{0.8}O_3$ and $CaSb_{0.25}Mn_{0.75}O_3$, respectively.

For all the solid solutions, the paramagnetic susceptibilities in the temperature range 250–330 K were analyzed, employing the Curie–Weiss equation. The Curie constant for $CaSb_{0.1}Mn_{0.9}O_3$ yields a value of 4.27 μ_B for μ_{exp}, the spin angular moment per one manganese atom. The effective magnetic moment can also be calculated (μ_{calc}) from the values for the free ions, Mn^{4+} (3.87 μ_B) and Mn^{3+} (4.90 μ_B for high spin configuration), with the approximation that there is no magnetic interaction between the Mn^{4+} and the Mn^{3+}, and that Sb^{5+} ions are present in the structure. The calculated value of 4.36 μ_B is in good agreement with that of 4.27 μ_B estimated from the Curie–Weiss law. A similar exercise for spin angular moment for $CaSb_{0.5}Mn_{0.5}O_3$ gives a value of 5.18 μ_B, which is smaller than that of free-ion value of 5.61 μ_B, implying that the manganese ions are affected by the crystal field. The observed good agreement between experimental and calculated values of the magnetic moments for

Table 4
Results of the Rietveld refinement of $CaSb_{0.2}Mn_{0.8}O_3$ in the space group $P2_1/m$ (No. 11)

Atom	Site	x/a	y/b	z/c	B_{iso} (Å^2)	Occupancy
Ca1	2*e*	−0.013 (4)	0.25	−0.017 (3)	1.2 (1)[a]	1
Ca2	2*e*	0.512 (3)	0.25	0.4660 (3)	1.2 (1)[a]	1
Mn1/Sb1	2*b*	0.5	0	0	0.022 (6)[a]	0.8/0.2
Mn2/Sb2	2*c*	0	0	0.5	0.022 (6)[a]	0.8/0.2
O1	2*e*	−0.037 (8)	0.25	0.510 (6)	0.2 (2)[a]	1
O2	2*e*	0.554 (8)	0.25	−0.004 (7)	0.2 (2)[a]	1
O3	4*f*	0.279 (4)	0.047 (2)	0.249 (5)	0.2 (2)[a]	1
O4	4*f*	0.186 (4)	0.051 (3)	0.801 (4)	0.2 (2)[a]	1

Note. Lattice parameters (Å): $a = 5.3520(6)$, $b = 7.5199(8)$, $c = 5.3978(6)$, $\beta = 91.054(6)$. *R* factors (%): $R_{wp} = 7.6$, $R_p = 5.4$, $S = 2.97$ (Mo$K\alpha_1$ radiation, refinement program: Rietan-94).
[a] Parameters constrained to be equal.

Table 5
Results of the Rietveld refinement of $CaSb_{0.25}Mn_{0.75}O_3$ in the space group $P2_1/m$ (No. 11)

Atom	Site	x/a	y/b	z/c	B_{iso} (Å^2)	Occupancy
Ca1	2*e*	−0.001 (2)	0.25	0.033 (2)	0.98 (6)[a]	1
Ca2	2*e*	0.498 (2)	0.25	0.544 (2)	0.98 (6)[a]	1
Mn1/Sb1	2*b*	0.5	0	0	0.17 (5)[a]	0.75/0.25
Mn2/Sb2	2*c*	0	0	0.5	0.17 (5)[a]	0.75/0.25
O1	2*e*	−0.070 (5)	0.25	0.4827 (4)	0.5 (1)[a]	1
O2	2*e*	0.568 (4)	0.25	−0.010 (4)	0.5 (1)[a]	1
O3	4*f*	0.282 (3)	0.044 (2)	0.283 (3)	0.5 (1)[a]	1
O4	4*f*	0.193 (3)	0.04 (3)	0.794 (2)	0.5 (1)[a]	1

Note. Lattice parameters (Å): $a = 5.3859(3)$, $b = 7.5387(1)$, $c = 5.4348(1)$, $\beta = 91.470(3)$. *R* factors (%): $R_{wp} = 5.6$, $R_p = 3.9$, $S = 2.60$ (Mo$K\alpha_1$ radiation, refinement program: Rietan-94).
[a] Parameters constrained to be equal.

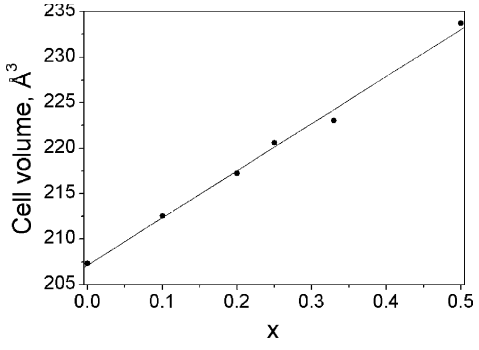

Fig. 5. Plot of unit cell volume against the Sb concentration (*x*) for $CaSb_xMn_{1-x}O_3$ ($x = 0$, 0.1, 0.2, 0.25, 0.33, 0.5) Datum for $x = 0$ was taken from [27].

samples with $x = 0.1$ and 0.5 suggests that Sb is in 5+ oxidation state in other solid solutions ($x = 0.2$, 0.25, 0.33) as well.

Similarly the values of 5.86, 5.73 and 5.41 μ_B were obtained for magnetic moment per manganese atom of solid solutions with $x = 0.2$, 0.25, 0.33, by employing the Curie–Weiss law in the temperature range 250–330 K. These values are much higher than the calculated values of 4.36, 4.44 and 4.70 μ_B, respectively. Though the temperature dependence of inverse magnetic susceptibility is linear for all these three samples in the temperature range 250–330 K (Fig. 7), the applicability of the Curie–Weiss law should be critically examined. Interactions between magnetic ions in this temperature range should be taken into consideration. Magnetic cluster formation can be supposed to take place in these cases. Sb^{5+} ions prevent long-range interactions, dividing the bulk material into smaller magnetic clusters. The average oxidation states of manganese in these three samples are close to 3.5+ and, therefore, the exchange interaction between Mn^{3+} and Mn^{4+} can play an important role. Deviation from this "optimal" oxidation state leads to decrease in spin angular moment. Precise information on cluster size and the cluster-size distribution cannot be derived in these compounds, in contrast to the molecular cluster compounds which consist of strictly identical particles. For instance the compound, $[Mn_{12}O_{12}(CH_3COO)_{16}(H_2O)_4] \cdot 2CH_3COOH \cdot 4H_2O$ ($Mn_{12}Ac$) contains 8 Mn^{3+} and 4 Mn^{4+} ions with an average oxidation state of 3.33+ for manganese [31]. These ions are magnetically coupled with an effective magnetic moment of 20.4 μ_B per cluster (or 5.89 μ_B per Mn atom) at low temperature and there are no interactions between clusters. The values of average manganese oxidation state and effective magnetic moment per Mn atom in $Mn_{12}Ac$ and $CaSb_xMn_{1-x}O_3$ ($x = 0.2$, 0.25, 0.33) are comparable. It should be noted

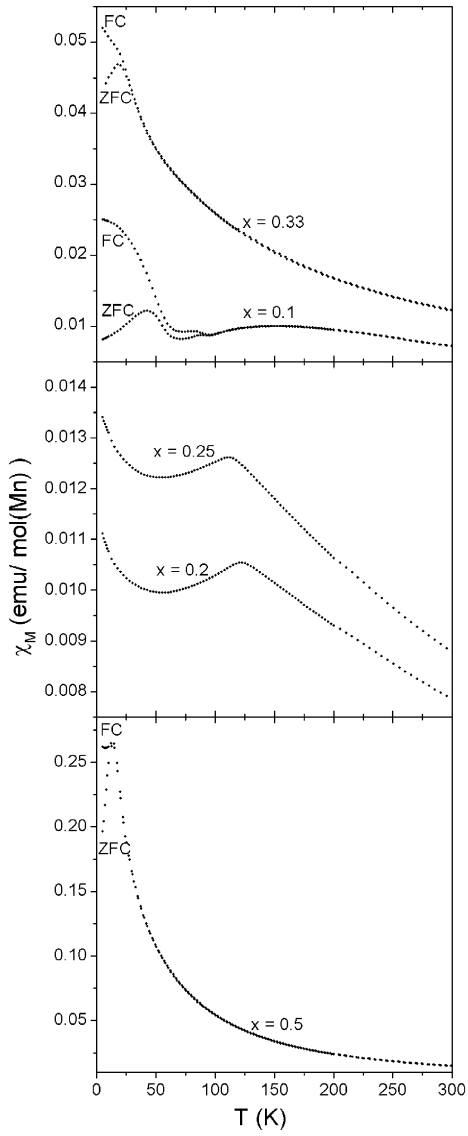

Fig. 6. A plot of magnetic susceptibility χ vs temperature for $CaSb_xMn_{1-x}O_3$ (ZFC—zero field cooling, FC—field cooling) in an applied magnetic field of 0.1 T.

that this similarity does not provide any information about cluster size in our compounds.

$CaSb_{0.5}Mn_{0.5}O_3$ is found to be an insulator whereas the other members, $CaSb_xMn_{1-x}O_3$ ($x = 0.1$, 0.2, 0.25, 0.33) exhibit semiconductor properties with room temperature resistivities of ca. 6×10^{-2}, 1.6, 3.5 and 100 Ω cm, respectively.

4. Conclusion

In conclusion, $CaSb_xMn_{1-x}O_3$ ($x = 0.1$, 0.2, 0.25, 0.33, 0.5) perovskite manganites have been synthesized by solid-state reaction. The Rietveld refinements of powder X-ray diffraction data indicate that $CaSb_{0.1}Mn_{0.9}O_3$

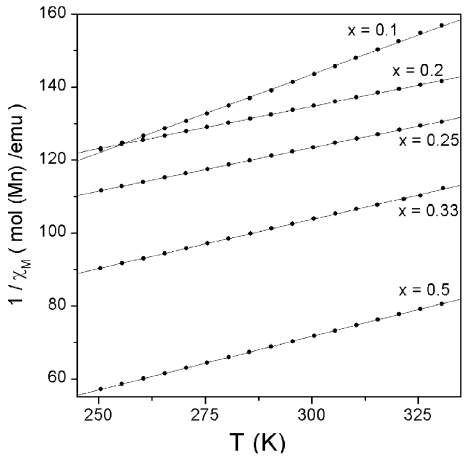

Fig. 7. Plot of $1/\chi$ against temperature for $CaSb_xMn_{1-x}O_3$ in the temperature range 250–330 K.

crystallizes with a *Pnma* orthorhombic structure, while $P2_1/m$ structure was adopted by the other members of the series. Linear dependence of cell volumes with concentration of Sb has been established. There is a divergence of the magnetic susceptibilities between ZFC and FC measurements for $CaSb_{0.1}Mn_{0.9}O_3$, $CaSb_{0.33}Mn_{0.67}O_3$ and $CaSb_{0.5}Mn_{0.5}O_3$ below 70, 25 and 14 K, respectively. $CaSb_{0.2}Mn_{0.8}O_3$ and $CaSb_{0.25}Mn_{0.75}O_3$ show antiferromagnetic transitions at 125 and 113 K, respectively. The results support the presence of magnetic clusters in these compounds.

Acknowledgments

V. Poltavets thanks the Alexander von Humboldt Foundation for financial support with a fellowship.

References

[1] C.N.R. Rao, A.K. Cheetham, R. Mahesh, Chem. Mater. 8 (1996) 2421–2432.
[2] R. von Helmolt, J. Wecker, B. Holzapfel, L. Schultz, K. Samwer, Phys. Rev. Lett. 71 (1993) 2331–2333.
[3] K. Chahara, T. Ohno, M. Kasai, Y. Kozono, Appl. Phys. Lett. 63 (1993) 1990–1992.
[4] A.J. Millis, P.B. Littlewood, B.I. Shraiman, Phys. Rev. Lett. 74 (1995) 5144–5147.
[5] P.G.d. Gennes, Phys. Rev. 118 (1960) 141–154.
[6] A. Moreo, S. Yunoki, E. Dagotto, Science 283 (1999) 2034–2040.
[7] E. Dagotto, T. Hottab, A. Moreo, Phys. Rep. 344 (2001) 1–153.
[8] S.J.L. Billinge, R.G. Difrancesco, G.H. Kwei, J.J. Neumeier, J.D. Thompson, Phys. Rev. Lett. 77 (1996) 715–718.
[9] G. Allodi, R. Derenzi, G. Guidi, F. Licci, M.W. Pieper, Phys. Rev. B: Condens. Matter Mater. Phys. 56 (1997) 6036–6046.
[10] J.W. Lynn, R.W. Erwin, J.A. Borchers, A. Santoro, Q. Huang, J.L. Peng, R.L. Greene, J. Appl. Phys. 81 (1997) 5488–5490.
[11] M. Uehara, S. Mori, C.H. Chen, S.W. Cheong, Nature 399 (1999) 560–563.

[12] M. Fath, S. Freisem, A.A. Menovsky, Y. Tomioka, J. Aarts, J.A. Mydosh, Science 285 (1999) 1540–1542.
[13] I.O. Troyanchuk, M.V. Bushinsky, H. Szymczak, K. Barner, A. Maignan, Eur. Phys. J. B 28 (2002) 75–80.
[14] A. Maignan, B. Raveau, Z. Phys. B: Condens. Mater. 102 (1997) 299–305.
[15] R. Laiho, K.G. Lisunov, E. Lahderanta, J. Salminen, V.S. Zakhvalinskii, J. Magn. Magn. Mater. 250 (2002) 267–274.
[16] C. Martin, A. Maignan, F. Damay, M. Hervieu, B. Raveau, Z. Jirak, G. Andre, F. Bouree, J. Magn. Magn. Mater. 202 (1999) 11–21.
[17] C. Martin, A. Maignan, M. Hervieu, B. Raveau, J. Hejtmanek, Eur. Phys. J. B 16 (2000) 469–474.
[18] A. Maignan, C. Martin, M. Hervieu, B. Raveau, J. Appl. Phys. 91 (2002) 4267–4270.
[19] A. Barnabe, A. Maignan, M. Hervieu, F. Damay, C. Martin, B. Raveau, Appl. Phys. Lett. 71 (1997) 3907–3909.
[20] A. Barnabe, A. Maignan, M. Hervieu, B. Raveau, Eur. Phys. J. B 1 (1998) 145–150.
[21] P.M. Woodward, Acta Crystallogr. B: Struct. Sci. 53 (1997) 32–43.
[22] J. Rodríguez-Carvajal, Physica B 192 (1993) 55–69.
[23] F. Izumi, in: R.A. Young (Ed.), The Rietveld Method, Oxford University Press, Oxford, 1993.
[24] H.M. Rietveld, J. Appl. Crystallogr. 2 (1969) 65–71.
[25] V. Primo-Martin, Powder Diffr. 14 (1999) 70.
[26] R.A. Young, in: R.A. Young (Ed.), The Rietveld Method, Oxford University Press, Oxford, 1993.
[27] H. Taguchi, M. Sonoda, M. Nagao, J. Solid State Chem. 137 (1998) 82–86.
[28] A.M. Glazer, Acta Crystallogr. B: Struct. Sci. 28 (1972) 3384–3392.
[29] R.D. Shannon, C.T. Prewitt, Acta Crystallogr. B: Struct. Sci. 25 (1969) 925–946.
[30] C.D. Ling, J.J. Neumeier, D.N. Argyriou, J. Solid State Chem. 160 (2001) 167–173.
[31] M.A. Novak, R. Sessoli, A. Caneschi, D. Gatteschi, J. Magn. Magn. Mater. 146 (1995) 211–213.